Numerical investigation of turbulent natural convection in enclosures

L. Škerget, J. Ravnik & J. Lupše
Faculty of Mechanical Engineering, University of Maribor, Maribor, Slovenia

Abstract

The set of partial differential equations governing the motion of viscous fluid is known as nonlinear Navier–Stokes equations. This equation system is generally considered to be the fundamental description for all laminar as well as turbulent flows. The occurrence of small scale structures in turbulent flows prevents a direct numerical simulation (DNS) of the governing Navier–Stokes equations. Therefore, much attention is paid to large eddy simulation (LES), in which the large scale turbulent structures are captured explicitly by the discretization model, while the effect of the small structures, namely subgrid scales, are modelled with an appropriate subgrid scale turbulent model. In the LES methodology the classical Smagorinsky subgrid scale eddy-viscosity model with Van Driest damping closed to the wall is most widely applied.

The paper deals with a LES numerical solver based on the velocity-vorticity formulation of the filtered Navier–Stokes equations. The governing equations are solved with a numerical solution algorithm, which is based on the boundary element method (BEM). The single domain as well as domain decomposition approaches are applied.
Keywords: Navier–Stokes equations, boundary element method, turbulence simulation and modelling, 2D DNS and LES numerical investigation, turbulent natural convection in enclosures.

1 Introduction

Natural convection in differentially heated enclosures is of importance in many engineering applications. At the same time the natural convection in a square cavity is also a very good and challenging benchmark example for numerical

WIT Transactions on Modelling and Simulation, Vol 54,
www.witpress.com, ISSN 1743-355X (on-line)
doi:10.2495/BEM130011

studies. The flow phenomena in the cavity are complicated specially when the fluid flow is turbulent. In numerical terms, the geometry of the cavity is simple and its boundary conditions are easy to determine. Therefore, natural convection in closed cavities enjoys permanent long-lasting attention from the experimental and numerical investigation aspects [1–3]. A numerical study of low-level turbulence natural convection in an air filled vertical square cavity was performed. The differentially heated cavity was of height $H = 1$ and width $W = H$. The hot and cold walls of the cavity were isothermal at relative temperature $T_h = +0.5$ and $T_c = -0.5$ resulting in a characteristic Rayleigh number value equal to $Ra = 10^9$.

The planar DNS and LES is used for velocity-vorticity formulation of the incompressible Navier–Stokes equations with the Boussinesq approximation for the buoyancy. The velocity-vorticity formulation in combination with the BEM is a promising, stable and very accurate numerical model for the numerical solution of general fluid flow problems [4–6]. Solution of the flow kinematics based on Biot–Savart law provides boundary vorticity values, leading to a well posed coupled vorticity transport equation. For the solution of domain velocity and vorticity values based on Poisson velocity equation and vorticity kinetic transport equation, respectively, a macro element model is applied [7].

2 Governing filtered flow equations

2.1 Primitive variables formulation

The governing equations for the filtered flow can be written in terms of effective momentum diffusivity ν_{ef} and thermal diffusivity a_{ef}, respectively, as follows

$$\mathrm{div}\overline{\vec{v}} = 0, \tag{1}$$

$$\rho_o \frac{D\overline{\vec{v}}}{Dt} = -\mathrm{rot}(\eta_{ef}\overline{\vec{\omega}}) + 2\mathrm{grad}\overline{\vec{v}} \cdot \mathrm{grad}\eta_{ef} + 2\mathrm{grad}\eta_{ef} \times \overline{\vec{\omega}} - \mathrm{grad}\overline{p}^{\star} + \overline{\rho}\vec{g}\,, \tag{2}$$

$$c_o \frac{D\overline{T}}{Dt} = \mathrm{div}\left(c_o a_{ef}\mathrm{grad}\overline{T}\right) + \overline{S_T}, \tag{3}$$

where the effective transport coefficient for the filtered flow equations are given by the definitions, e.g. $\nu_{ef} = \nu + \nu_s$ and $a_{ef} = a + a_s$, respectively. The modified filtered pressure term $\overline{p}^{\star}$ represents the sum of the static pressure and the trace of subgrid-scale stress tensor, respectively, such as

$$\overline{p}^{\star} = \overline{p} + \frac{1}{3}\rho_o \tau_{kk}^{R}. \tag{4}$$

The effective viscosity η_{ef} and effective heat conductivity k_{ef} can be given as a sum of a constant and variable part

$$\eta_{ef} = \eta_{efo} + \widetilde{\eta_{ef}} \quad , \quad k_{ef} = k_{efo} + \widetilde{k_{ef}}\,, \tag{5}$$

therefore the momentum and energy equations (2) and (3) can be written in analogy to the basic conservation equations formulated for the constant material properties

$$\rho_o \frac{D\overline{\vec{v}}}{Dt} = -\eta_{efo}\mathrm{rot}\overline{\vec{\omega}} - \mathrm{grad}\overline{p}^{\star} + \overline{\rho}\vec{g} + \overline{\vec{f}^{m}}, \quad c_o \frac{D\overline{T}}{Dt} = k_{efo}\triangle\overline{T} + \overline{S_T} + \overline{S_T^m}\,, \tag{6}$$

where the pseudo body force term $\overline{\vec{f}^{m}}$ and pseudo heat source term $\overline{S_T^m}$, are introduced into the momentum and energy equations (6), respectively, capturing the variable transport property effects, and given by expressions

$$\overline{f_i^m} = -e_{ijk}\frac{\partial\overline{\omega_k}}{\partial x_j}\widetilde{\eta_{ef}} + e_{ijk}\frac{\partial\eta_{ef}}{\partial x_j}\overline{\omega_k} + 2\frac{\partial\eta_{ef}}{\partial x_j}\frac{\partial\overline{v_i}}{\partial x_j}, \quad \overline{S_T^m} = \frac{\partial}{\partial x_j}\left(\widetilde{k_{ef}}\frac{\partial\overline{T}}{\partial x_j}\right). \tag{7}$$

2.2 Velocity-vorticity filtered flow formulation

With the filtered vorticity vector $\overline{\omega_i}$ representing the curl of the velocity field $\overline{v_i}$ the fluid motion computation scheme is partitioned into its kinematics, given by the elliptic filtered velocity vector equation

$$\frac{\partial^2\overline{v_i}}{\partial x_j\partial x_j} + e_{ijk}\frac{\partial\overline{\omega_k}}{\partial x_j} = 0\,, \tag{8}$$

or in its parabolised false transient form

$$\frac{\partial^2\overline{v_i}}{\partial x_j\partial x_j} - \frac{1}{\alpha}\frac{\partial\overline{v_i}}{\partial t} + e_{ijk}\frac{\partial\overline{\omega_k}}{\partial x_j} = 0\,, \tag{9}$$

where α is a relaxation parameter, to increase the stability of the computation scheme, and kinetics given by filtered vorticity transport equation, obtained as a curl of the filtered momentum eq. (6), e.g., written for two-dimensional plane flow case as the following scalar filtered vorticity statement

$$\frac{\partial\overline{\omega}}{\partial t} + \frac{\partial\overline{v_j}\,\overline{\omega}}{\partial x_j} = \nu_{efo}\frac{\partial^2\overline{\omega}}{\partial x_j\partial x_j} - \frac{1}{\rho_o}e_{ij}\frac{\partial\overline{\rho}g_i}{\partial x_j} - \frac{1}{\rho_o}e_{ij}\frac{\partial\overline{f_i^m}}{\partial x_j}\,. \tag{10}$$

2.3 Subgrid-scale closure/modelling

One of the most popular Boussinesq eddy-viscosity subgrid closure model is due to Smagorinsky, e.g. which correlates τ_{ij}^R to the large-scale strain-rate tensor $\overline{\dot{\varepsilon}_{ij}}$ [6,8]

$$\tau_{ij}^R = -2\eta_s\overline{\dot{\varepsilon}_{ij}} + \frac{1}{3}\rho_o\tau_{kk}^R\delta_{ij}\,. \tag{11}$$

The subgrid viscosity ν_s can be expressed as

$$\nu_s = (C_s l_s)^2\overline{\dot{\gamma}} \qquad \text{and} \qquad l_s = \triangle = (\triangle\Omega)^{1/3}, \tag{12}$$

where C_s is the Smagorinsky constant, l_s is the length scale of the unresolved flow, $\triangle\Omega$ is the volume of the computational internal cell and $\overline{\dot{\gamma}}$ is the deformation

velocity of the resolved flow $\overline{\dot{\varepsilon}_{ij}}$. The correct distribution of C_s in the near wall region is obtained by using so-called damping functions, e.g. the most often used is the van Driest damping function

$$C_s = C_{so}\left(1 - \exp(-Re_\tau/25)\right)^2. \tag{13}$$

The subgrid-scale heat flux $\overline{v_j T}$, that appeared in eq. (6), can be modelled as simple gradient diffusion hypothesis

$$\overline{v_j T} = -\frac{\nu_s}{Pr_t}\frac{\partial \overline{T}}{\partial x_j}, \tag{14}$$

where Pr_t is the turbulent Prandtl number.

3 Boundary-domain integral equations

The kinematics of plane motion is given by two scalar equations as follows [5]:

$$c\left(\xi\right)\overline{v_i}\left(\xi\right) + \int_\Gamma \overline{v_i} q^\star d\Gamma = \int_\Gamma \frac{\partial v_i}{\partial n} u^\star d\Gamma + e_{ij}\int_\Gamma \overline{\omega} n_j u^\star d\Gamma - e_{ij}\int_\Omega \overline{\omega} q_j^\star d\Omega. \tag{15}$$

where $u^\star$ stands for the elliptic Laplace fundamental solution and $q^\star$ is its normal derivative, or in its parabolic formulation

$$c\left(\xi\right)\overline{v_i}\left(\xi, t_F\right) + \int_\Gamma \overline{v_i} Q^\star d\Gamma = \int_\Gamma \frac{\partial v_i}{\partial n} U^\star d\Gamma$$
$$+e_{ij}\int_\Gamma \overline{\omega} n_j U^\star d\Gamma - e_{ij}\int_\Omega \overline{\omega} Q_j^\star d\Omega + \int_\Omega \overline{v_i}_{F-1} u^\star d\Omega, \tag{16}$$

with $u^\star$ stands now for the parabolic diffusion fundamental solution [9] and $U^\star$ represents its time integral over time increment.

Accounting for the compatibility and restriction conditions for velocity and vorticity fields to eq. (15), the following boundary integral representation for the general flow situation can be stated for the two-dimensional plane flow kinematic case as follows

$$c\left(\xi\right)\overline{v_i}\left(\xi\right) + \int_\Gamma \overline{v_i} q^\star d\Gamma = e_{ij}\int_\Gamma \overline{v_j} q_t^\star d\Gamma - e_{ij}\int_\Omega \overline{\omega} q_j^\star d\Omega\,, \tag{17}$$

known as Biot–Savart law. Using unique feature of global integral representation for boundary vorticity values, the vector eq. (17) has to be written in its tangential form.

With the use of the linear parabolic diffusion operator the vorticity equation can be given as:

$$c\left(\xi\right)\overline{\omega}\left(\xi,t_F\right)+\int_{\Gamma}\overline{\omega}Q^{\star}d\Gamma=\frac{1}{\eta_o}\int_{\Gamma}\left(\eta_o\frac{\partial\overline{\omega}}{\partial n}-\rho_o v_n\overline{\omega}+\rho g_t\right)U^{\star}d\Gamma$$

$$+\frac{1}{\eta_o}\int_{\Omega}\left(\rho_o\overline{v_j\omega}+e_{ij}(\rho g_i+\overline{f_i^m})\right)Q_j^{\star}d\Omega+\int_{\Omega}\overline{\omega}_{F-1}u_{F-1}^{\star}d\Omega, \qquad (18)$$

where a constant variation of all field functions within the individual time increment is assumed, e.g. the values at $t=t_F$ are considered for each time step, where v_n and g_t are the normal velocity, and the tangential gravity, respectively, e.g. $v_n=\vec{v}\cdot\vec{n}$, $g_t=\vec{g}\cdot\vec{t}=-e_{ij}g_in_j$. The integral representation of the heat energy equation can be formulated as

$$c\left(\xi\right)\overline{T}\left(\xi,t_F\right)+\int_{\Gamma}\overline{T}Q^{\star}d\Gamma=\frac{1}{k_o}\int_{\Gamma}\left(k_o\frac{\partial\overline{T}}{\partial n}-c_o\overline{v_n}\overline{T}\right)U^{\star}d\Gamma$$

$$+\frac{1}{k_o}\int_{\Omega}(c_o\overline{v_j}\overline{T}+\overline{S_T^m})Q_j^{\star}d\Omega+\int_{\Omega}\overline{T}_{F-1}u_{F-1}^{\star}d\Omega\,. \qquad (19)$$

4 Numerical aspects/iterative strategy

The main advantages of the Smagorinsky model are its simplicity and its stability. Whether filtering is introduced or not, the LES equations with subgrid-scale eddy viscosity model are solved numerically for the time evolution of the LES field functions. This involves discretization in space and time, which introduces differences between the differential equations and their numerical equivalent. The solution iterative strategy is to solve for large scale velocity $\vec{v}$ and vorticity $\vec{\omega}$ field functions and then to compute subgrid-scale eddy viscosity until convergence, repeating the iterative process if needed. The solution scheme is as follows:

1. Solve the filtered Navier–Stokes LES equations
   1.1 Update subgrid-scale eddy viscosity ν_s
2. Check convergence for $\vec{\omega}$. If not, go to 1.

5 Onset of unsteady turbulent natural convection in an differentially heated square cavity

We consider a square cavity of height $H=1$ and width $W=H$, filled with a Newtonian viscous fluid. It is submitted to a temperature difference $\triangle T=T_h-T_c>0$ at the vertical walls, with uniform temperatures $T_h=0.5$ and $T_c=-0.5$, respectively, while the top and bottom walls are adiabatic, Fig. 1. A non-uniform symmetric mesh of $M=80\times80$ elements is used, with the ratio $R=10$ between the largest and the smallest boundary element. The mesh features

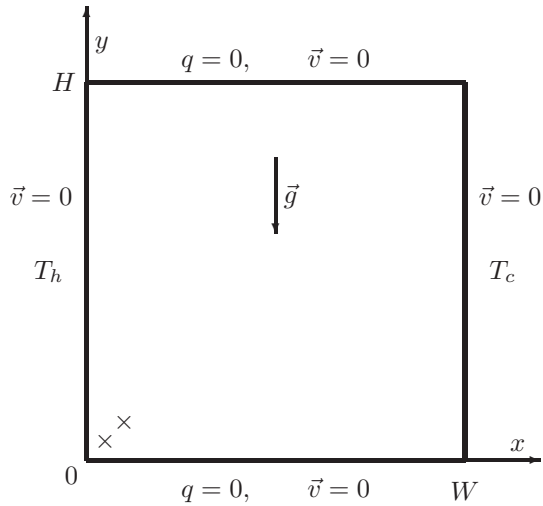

Figure 1: Boundary and initial conditions for the simulation of natural convection flow in a square cavity; the left wall is heated and kept at uniform temperature $T_h = 0.5$, while the right wall is cooled and kept at $T_c = -0.5$. $\times$ denotes location of points from where time traces and phase portraits are extracted.

320 boundary elements, 6400 boundary nodes and the total number of nodes is 25921. Convergence criterion was selected as $\epsilon = 10^{-6}$. The time-dependent analysis was performed by running the simulation from the initial state with a time step value of $\triangle t = 1 \times 10^{-6}$.

Turbulent natural convection in a differently heated air-filled square cavity with adiabatic horizontal walls is investigated by direct numerical simulation DNS and large eddy simulation LES numerical integration of the unsteady two-dimensional governing equations. In order to approach chaotic flows which exhibits randomness in space as well as in time, simulations for Rayleigh number value $Ra = 1 \times 10^9$ and Prandtl number value $Pr = 0.71$ are performed. It is necessary to integrate the unsteady governing equations long enough in time so that the transient effects have died out and the asymptotic behaviour is reached.

Instantaneous temperature and vorticity fields obtained by DNS simulation are shown in Fig. 2 and Fig. 3 for Rayleigh number value $Ra = 1 \times 10^9$. Filtered temperature and vorticity fields obtained by LES simulation are shown in Fig. 4 and Fig. 5 for Rayleigh number value $Ra = 1 \times 10^9$. Examining the flow fields gives an impression of wide variety of scales in the flow fields. Fig. 6 shows the oscillatory nature of temperature versus time for DNS and LES damping results. The transition from oscillatory to chaotic flow circumstances can also be observed in temperature-vorticity phase portraits, Fig. 7. Sajjadi *et al.* [10] used the lattice Boltzmann method to simulate turbulent natural convection with LES. They reported that the average Nusselt number at $Ra = 10^9$ is $Nu = 58.1$. We

plot the average Nusselt number time series of our results in Fig. 8. The time series of our results is still too short and the flow did not reach a self similar state, where a time average value could be calculated.

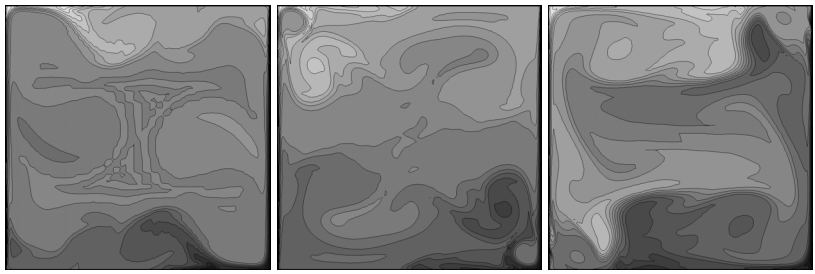

Figure 2: DNS instantaneous temperature fields for $Ra = 1 \times 10^9$ at $t = 8 \cdot 10^{-4}$ (left), $t = 16 \cdot 10^{-4}$ (middle), $t = 24 \cdot 10^{-4}$ (right).

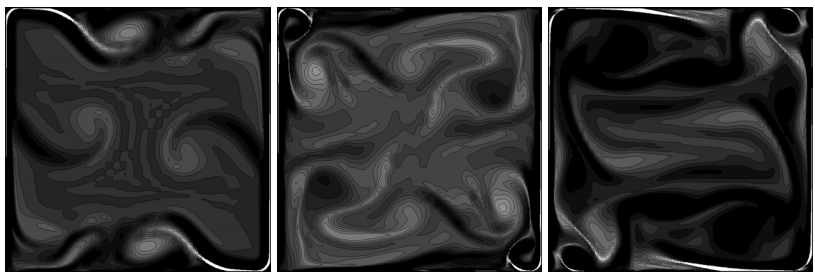

Figure 3: DNS instantaneous vorticity fields for $Ra = 1 \times 10^9$ at $t = 8 \cdot 10^{-4}$ (left), $t = 16 \cdot 10^{-4}$ (middle), $t = 24 \cdot 10^{-4}$ (right).

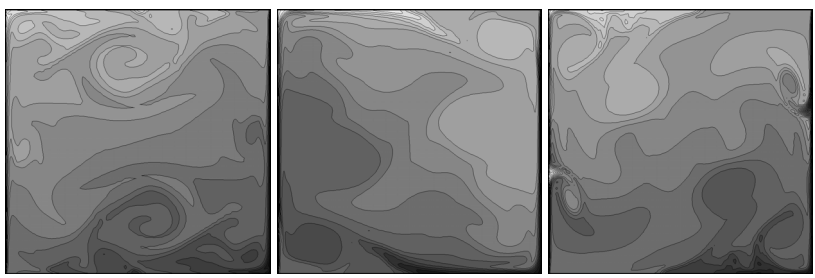

Figure 4: LES filtered temperature fields for $Ra = 1 \times 10^9$ at $t = 8 \cdot 10^{-4}$ (left), $t = 10 \cdot 10^{-4}$ (middle), $t = 12 \cdot 10^{-4}$ (right).

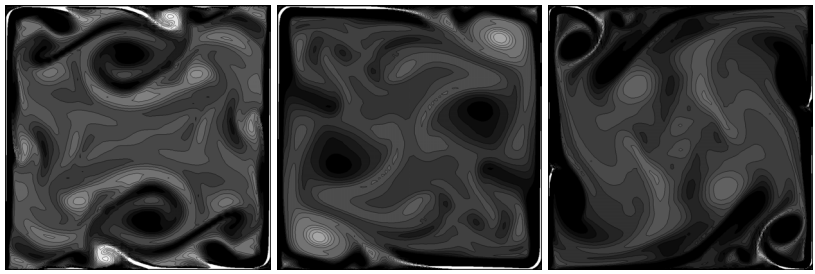

Figure 5: LES filtered vorticity fields for $Ra = 1 \times 10^9$ at $t = 8 \cdot 10^{-4}$ (left), $t = 10 \cdot 10^{-4}$ (middle), $t = 12 \cdot 10^{-4}$ (right).

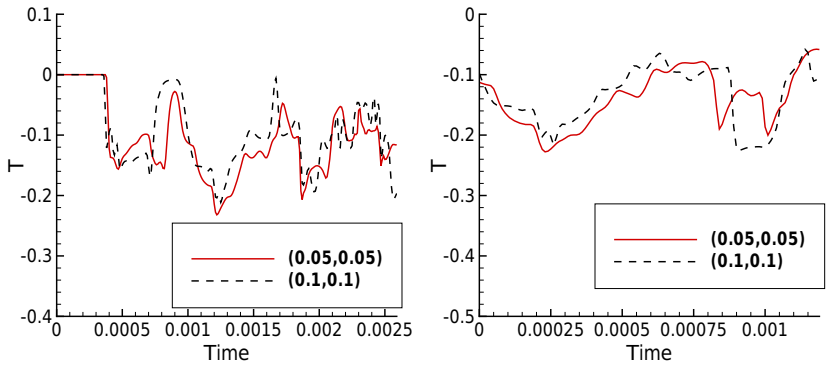

Figure 6: Time traces of temperature for $Ra = 1 \times 10^9$ for DNS (left) and LES (right) at two specific locations in the bottom left corner of the cavity.

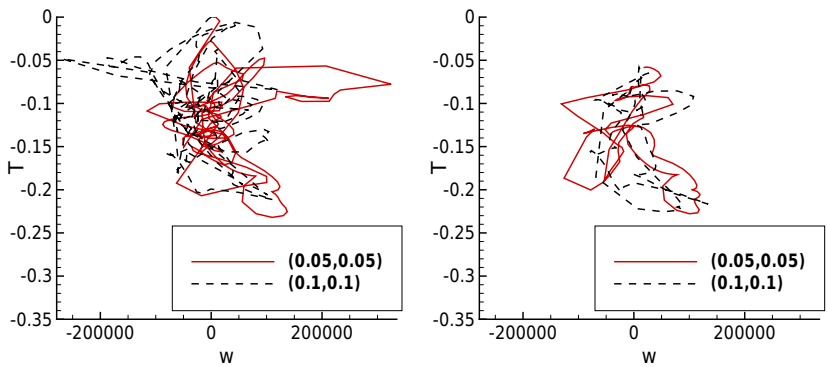

Figure 7: Temperature-vorticity time series phase portraits for $Ra = 1 \times 10^9$ for DNS (left) and LES (right).

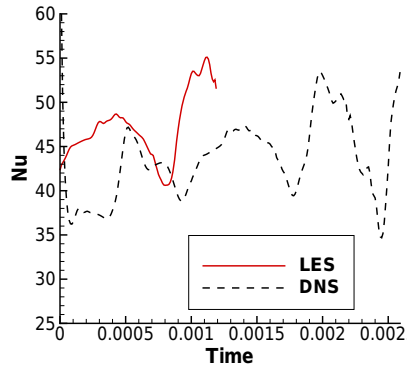

Figure 8: Average heat flux through the vertical wall expressed in term of the Nusselt number, $Ra = 1 \times 10^9$.

6 Conclusions

The velocity-vorticity formulation of DNS and LES based BEM presented in this paper shows good potential for solving general turbulent transport phenomena. Relatively dense meshes can be used by the use of domain decomposition technique. False transient approach to kinematics considerably increases the stability of the numerical algorithm at high Rayleigh number values. To increase the accuracy and the stability of the developed numerical model higher order time integration schemes will be introduced, e.g. linear approximation of all field functions over each individual time step.

In this work a numerical procedure based on the boundary element method for the simulation of unsteady turbulent buoyancy-driven two-dimensional fluid flow in a differentially heated air-filled cavity is investigated. The flow circumstances for different Rayleigh number values of $Ra = 1 \times 10^9$ is studied. Relatively coarse nonuniform meshes are used in the numerical model. The transition to turbulent flow was investigated by studying time series plots, power spectra and vorticity-temperature phase diagrams. Rather large fluctuations are observed in the cavity corners. With increasing Ra the cavity core becomes deorganised and chaotic.

References

[1] Xin, S. and Le Quere, P.: *Direct numerical simulations of two-dimensional chaotic natural convection in a differently heated cavity of aspect ratio 4*. J. Fluid Mech., Vol.304, pp.87–118, (1995).

[2] Ampofo, F., Karayiannis, T.G.: *Experimental benchmark data for turbulent natural convection in an air filled square cavity*. Int. J. Heat and Mass Transfer, 46, pp.3551–3572, (2003).

[3] Salat, J., Xin, S., Joubert, P., Sergent, A., Penot, F., Le Quere, P.: *Experimental and numerical investigation of turbulent natural convection in a large air-filled cavity*. Int. J. Heat and Fluid Flow, 25, pp.824–832, (2004).
[4] Ingber, M.: *A vorticity method for the solution of natural convection flows in enclosures*. Int. J. Numer. Methods Heat Fluid Flow, 13, pp.655–671, (2003).
[5] Škerget, L., Hriberšek, M., Kuhn, G.: *Computational fluid dynamics by boundary domain integral method*. Int. J. Numer. Meth., 46, pp.1291–1311, (1999).
[6] Ravnik, J., Škerget, L., Hriberšek, M.: *Two-dimensional velocity-vorticity based LES for the solution of natural convection in a differentially heated enclosure by wavelet transform based BEM and FEM*. Eng. Anal. Bound. Elem., 30, pp.671–686, (2006).
[7] Ramšak, M., Škerget, L.: *A subdomain boundary element method for high-Reynolds laminar flow using stream function-vorticity formulation*. Int. J. Numer. Meth., 46, pp.815–847, (2004).
[8] Biswas, G. and Eswaran, V. (eds.): *Turbulent Flows: Fundamentals, Experiments and Modeling*. Alpha Science International Ltd., Pangbourne, United Kingdom, (2002).
[9] Škerget, L., Brebbia, C.A.: *Time dependent non-linear potential problems*. Ch. 3: Progress in Boundary Element Methods, Vol.3, Springer-Verlag, Berlin, Heidelberg, New York, (1984).
[10] Sajjadi H., Gorji M., Kefayati GH.R., Ganji D.D. and Shayan Nia M.: *Numerical Analysis of Turbulent Natural Convection in a Square Cavity using Large eddy Simulation in Lattice Boltzmann Method*. World Academy of Science, Engineering and Technology 61, pp.819–823, (2012).